THE JOURNAL OF BIOLOGICAL CHEMISTRY VOL. 286, NO. 2, pp. 1389–1399, January 14, 2011

Intracellular Regions of the Eag Potassium Channel Play a Critical Role in Generation of Voltage-dependent Currents*[S]

Received for publication, September 11, 2010, and in revised form, November 4, 2010 Published, JBC Papers in Press, November 8, 2010, DOI 10.1074/jbc.M110.184077

Yong Li[‡§1,2], **Xinqiu Liu**[‡§1], **Yuying Wu**[‡1], **Zhe Xu**[‡], **Hongqin Li**[‡], **Leslie C. Griffith**[¶], **and Yi Zhou**[‡3]

From the [‡]*Department of Biomedical Sciences, Florida State University College of Medicine, Tallahassee, Florida 32306, the* [§]*Department of Neurobiology, Shanghai Jiao Tong University School of Medicine, Shanghai 200025, China, and the* [¶]*Department of Biology and Center for Complex Systems, Brandeis University, Waltham, Massachusetts 02454*

Folding, assembly, and trafficking of ion channels are tightly controlled processes and are important for biological functions relevant to health and disease. Here, we report that functional expression of the Eag channel is temperature-sensitive by a mechanism that is independent of trafficking or surface targeting of the channel protein. Eag channels in cells grown at 37 °C exhibit voltage-evoked gating charge movements but fail to conduct K^+ ions. By mutagenesis and chimeric channel studies, we show that the N- and C-terminal regions are involved in controlling a step after movement of the voltage sensor, as well as in regulating biophysical properties of the Eag channel. Synthesis and assembly of Eag at high temperature disrupt the ability of these domains to carry out their function. These results suggest an important role of the intracellular regions in the generation of Eag currents.

Voltage-gated K^+ channels consist of a large family of proteins that selectively conduct potassium ions when activated by changes of membrane potential (1). They consist of four subunits, each containing six transmembrane segments (S1–S6) that assemble together to form the voltage sensor and central pore domains (2, 3). It is now well established that opening of these channels is initiated by conformational changes of the voltage sensor domains upon membrane depolarization. Little, however, is known regarding the molecular and physical mechanisms underlying the coupling between the voltage sensor and activation gate of these K^+ channels (4). Voltage-gated K^+ channels diverge significantly in their N- and C-terminal (NT[4] and CT) regions, and for many channels these domains have been shown to be important for binding of auxiliary subunits or modulators (5). The roles of intracellular domains in gating, activation, and inactivation are less well understood (6–8).

The *Drosophila ether-à-go-go* channel (Eag) is the founding member of an evolutionarily conserved subfamily of voltage-gated K^+ channels, which includes hERG (human *eag*-related gene), a channel that plays an important role in regulating cardiac excitability and maintaining normal cardiac rhythm (9, 10). hERG channel dysfunction is responsible for a third of the congenital long QT syndrome and the vast majority of drug-induced long QT (10). In flies, mutation of *eag* increases neuronal excitability and affects memory formation (11, 12). This family of channels is therefore critical to the function of multiple types of excitable cells across the animal kingdom.

Structurally, Eag family channels are related to both voltage-gated K^+ channels and cyclic nucleotide-gated cation channels as they not only have transmembrane domains for voltage sensing and K^+ ion permeation but also contain a cyclic nucleotide-binding motif within their C-terminal regions (13, 14). Although Eag family channels may not be directly gated by cyclic nucleotides, several lines of evidence have suggested their NT and CT domains are important to channel function. First, mutations in these regions can result in defective synthesis, trafficking, or gating of the channels. Such mutations in hERG channels are one of the most prevalent causes of congenital human long QT syndrome (15, 16). Second, Eag channel activity and/or surface expression are regulated by a number of signaling molecules through direct binding to the NT and CT domains (17–20). Moreover, the *eag* transcript can be alternatively spliced to produce a protein that contains only the NT and CT regions and modulates cellular signal transduction pathways (21).

In this study, we report a direct involvement of these intracellular regions in the activation of Eag K^+ channels. Our data reveal that, in heterologous expression systems, the NT and CT regions of Eag are critical for functional expression of K^+ currents, specifically processes following movement of the voltage-sensing domain.

EXPERIMENTAL PROCEDURES

Plasmids and Construction—The cDNA encoding *Drosophila* Eag (kindly provided by Dr. Gisela Wilson, University of Wisconsin, Madison) was subcloned into a mammalian expression vector, pcDNA3. The myc-*eag* and *eag*-EGFP cDNAs were constructed by either cloning the *eag* coding sequence into the pCS2 vector containing six Myc epitopes or fusing EGFP to the C terminus of the *eag* coding region in the pEGFP-N1 vector. To measure surface expression of Eag proteins, a Myc tag was inserted in the extracellular loop that

* This work was supported, in whole or in part, by National Institutes of Health grant (to Irwin B. Levitan) and Grants NS50355 (to Y. Z.) and GM54408 (to L. C. G.).

[S] The on-line version of this article (available at http://www.jbc.org) contains supplemental Figs. S1 and S2.

[1] These authors contributed equally to this work.
[2] To whom correspondence may be addressed. Tel.: 86-21-64665820; Fax: 86-21-64453296; E-mail: liyong68@shsmu.edu.cn.
[3] To whom correspondence may be addressed. Tel.: 850-645-8217; Fax: 850-644-5781; E-mail: yzhou@fsu.edu.

[4] The abbreviations used are: NT, N-terminal; CT, C-terminal; mEag, mouse homologue of Eag; TM, transmembrane; hERG, human *eag*-related gene; ANOVA, analysis of variance; EGFP, enhanced GFP; pF, picofarad; TEA, tetraethylammonium.

connects transmembrane domains S1 and S2 of the Eag channel (Eag-EX-myc). The insertion changes the amino acid sequence between S1 and S2 to ^{255}PYNVAFK**EQKLISEEDL**NKTSEDVS, in which the Myc epitope is shown in boldface type. The chimeric Eag-mEag channels (Eag-NTmEag, Eag-CTmEag, or Eag-S1-S6mEag) were created by replacing the N- and C-terminal tails or transmembrane region of *Drosophila* Eag (residues 1–211, 501–1174, or 212–500) with the corresponding region of the mouse Eag channel (residues 1–192, 509–987, or 193–508). A similar approach was utilized to generate N-terminal truncation mutants of Eag or mEag. The mEag NT domain (mEagNT(1–190)-HA) was cloned into the pIRES-EGFP vector. The C-terminal truncation mutants of wild-type Eag, mEag, or chimeric Eag were constructed by introducing a stop codon into the cDNA at appropriate locations using the QuikChange strategy (Stratagene). All cDNA constructs were verified by DNA sequencing in the Florida State University Biology Sequencing Facility, Tallahassee, FL.

Biotinylation of Cell-surface Proteins—*eag*-pcDNA3 was transiently expressed in tsA 201 cells using a calcium phosphate-mediated transfection protocol. 2 days after transfection, cells were incubated with 0.5 mg/ml EZ-link-Sulfo-NHS-LC-biotin (Pierce) in PBS, pH 8.0, at room temperature for 30 min with gentle agitation. After removing the reagent by washing cells three times with PBS, cells were harvested and lysed using standard protocols (22). Biotinylated proteins were precipitated from cell lysates with ImmunoPure streptavidin beads (Pierce). Channel proteins in total cell lysates and streptavidin precipitates were analyzed by immunoblot using an affinity-purified anti-Eag antibody as described previously (20). To confirm that the biotinylation reagent did not leak into the cell and label intracellular proteins, we stripped and reprobed the same blots with an anti-GAPDH antibody (En-Cor Biotechnology, Inc.). Immunoblot images were quantified using ImageJ 1.43 (rsb.info.nih.gov).

Confocal Microscopy—tsA 201 or Chinese hamster ovary (CHO) cells were grown on poly-L-lysine-treated cover glasses and transfected with *eag*-EX-myc cDNAs. To label cell surface Eag proteins, cells were first incubated with 20 μg/ml anti-Myc antibody (Millipore) for 30 min at 37 °C, then fixed with 4% paraformaldehyde in PBS (30 min), blocked in 5% goat serum in PBS with 0.1% Triton X-100 (30 min), and labeled with FITC-conjugated anti-mouse antibody (2 h). To visualize total Eag proteins, transfected cells were first fixed and permeabilized with 0.2% Triton and then incubated with anti-Eag antibody and FITC-conjugated anti-rabbit antibody in the presence of 10% goat serum. Fluorescence images were acquired with a Leica TCS SP2 AOBS laser confocal microscope and analyzed using the ImageJ 1.43 software.

Electrophysiology—Ionic and gating currents of Eag channels were measured in the whole-cell configuration from CHO or tsA 201 cells transiently transfected with various *eag* cDNAs along with the pEGFP-N1 vector cDNA (Clontech) in a 9:1 ratio using either the FuGENE 6 (for tsA 201 cells; Roche Applied Science) or Lipofectamine LTX (for CHO cells; Invitrogen) transfection reagents. Transfected cells bearing GFP fluorescence were identified with a FITC filter set on a TE2000U inverted fluorescence microscope (Nikon). Patch electrodes with resistances of 2–4 megohms were pulled from borosilicate glass and fire-polished. Ionic and gating currents were digitized at 20 kHz and filtered at 1 and 5 kHz, respectively, with an Axopatch 200B amplifier. Data acquisition and analysis were performed with pCLAMP10 software (Molecular Devices). To record gating currents, a P/4 protocol was applied on line to subtract leak and capacitive currents (23).

For ionic K^+ current recording, the standard bath solution contained 2 mM KCl, 148 mM NaCl, 2 mM $MgCl_2$, 10 mM HEPES, and 1 mM EGTA, pH 7.4. The pipette solution contained 130 mM KCl, 10 mM HEPES, and 5 mM EGTA, pH 7.4. For gating currents measurements, the extracellular Na^+ and intracellular K^+ ions were replaced with equal molar of either NMG^+ or TEA-Cl. Recordings were generally conducted at room temperature. In experiments involving acute temperature changes, the bath temperature was maintained by a heated stage with the temperature controller, TC-344B (Warner Instruments).

The channel conductance was determined by measuring the amplitudes of isochronal tail currents evoked by repolarizing to −60 mV from various depolarizing potentials. Tail current amplitudes were normalized to the maximum value obtained in the experiment and plotted *versus* depolarizing potentials. Data were fitted with a single Boltzmann function using Origin 7.0 (Origin Lab, Northampton, MA). Deactivation kinetics was measured by fitting the tail currents with a single exponential function to obtain values for the deactivation time constant (τ_{deact}) using the Clampfit 10 program (Molecular Devices). As Eag channel currents display the sigmoid rise phase, activation kinetics was quantified by measuring the time to half-maximal current amplitude ($t_{½}$) at a depolarizing potential of +60 mV.

Temperature Change Protocol—tsA 201 or CHO cells were maintained at 37 °C. For experiments performed at 26 °C, cells were kept at 37 °C for 24 h following transfection and then switched to an incubator maintained at 26 °C.

Data Analysis—The majority of data were analyzed statistically by one-way ANOVA using Origin 7 software. Statistical significance was set at $p < 0.05$. To compare the probability of gating currents occurrence between groups, we used standard logistic regression analysis using the statistical software R-2.11.1.

RESULTS

Functional Expression of Recombinant Eag K^+ Channels Is Dependent upon Cultivation Temperature—Eag produces voltage-dependent outward K^+ currents when expressed in *Xenopus* oocytes (24). In contrast, when *eag* cDNA is transfected into cultured mammalian cells, no significant macroscopic K^+ current is elicited by depolarizing voltage steps from either transfected CHO or tsA 201 cells (Fig. 1, *A* and *B, left panels*). Mammalian cell lines differ from *Xenopus oocytes* in their culture temperature (37 °C), which is known to affect trafficking and/or surface targeting of some ion channels, including mutant hERG channels (25–28). To determine whether temperature was affecting current levels, we measured whole-cell K^+ currents from mammalian cells that were cultivated at lower temperatures after transfection with *eag*

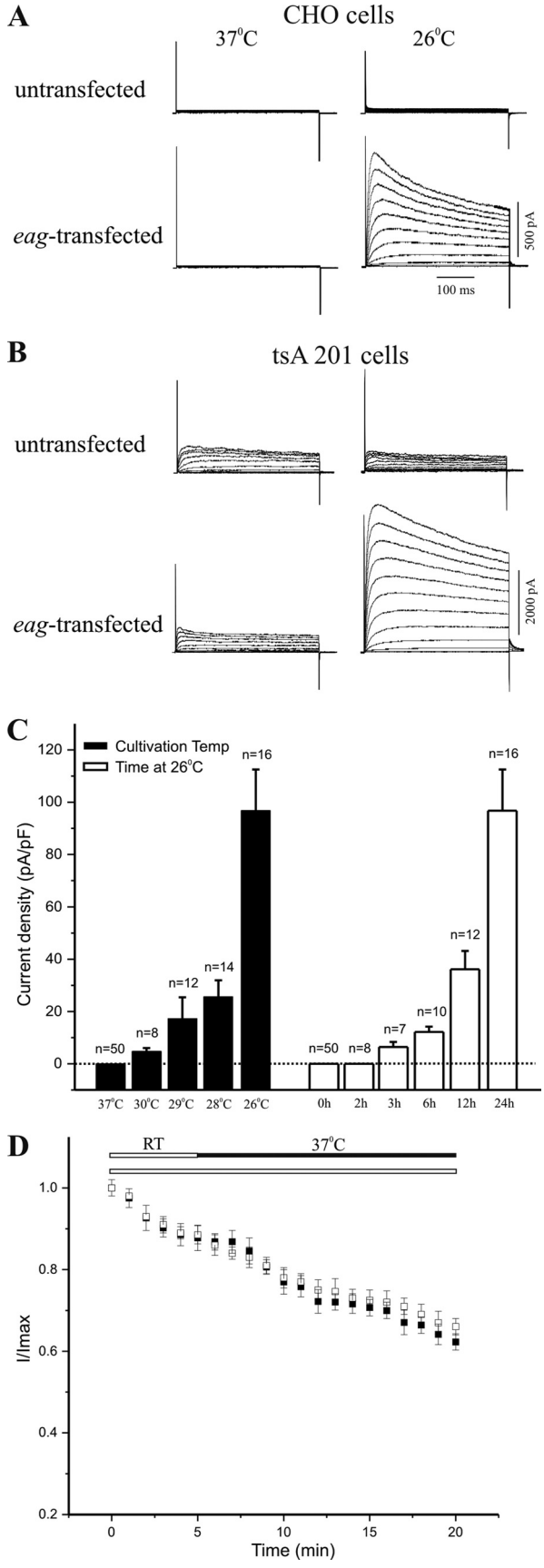

FIGURE 1. **Temperature-dependent expression of Eag K^+ currents in transfected cells.** Representative traces of whole-cell K^+ currents recorded from untransfected or *eag*-transfected CHO (*A*) and tsA 201 (*B*) cells cultivated at either 37 °C (*left*) or 26 °C (*right*). Currents were evoked by a series of 400-ms depolarizing voltage steps to +50 mV in 10-mV increments from a holding potential of −80 mV. Note that there were endogenous outward K^+ currents in untransfected tsA 201 (*B, top traces*) but not in CHO cells (*A, top traces*) (46) cultivated at either 37 or 26 °C. *C,* quantification of the effect of cultivation temperatures and durations at 26 °C on expression of Eag K^+ currents, as compared with current density (mean ± S.E.) at +40 mV from *eag*-transfected CHO cells that were either cultivated at 26 °C for various durations or at various temperatures for 24 h. *Dotted line* indicates current density of zero. *D,* recording at 37 °C does not abolish Eag K^+ currents. Cells were repeatedly depolarized to +40 mV from a holding potential of −80 mV. *Solid bar* denotes the period during which recording temperature was raised to 37 °C, and data at this condition are represented by *filled squares* (mean ± S.E., $n = 3$). There was a comparable rundown of Eag currents when recordings were conducted throughout at room temperature (*RT*, 22–25 °C), as indicated by an *open bar* and data shown with *open squares* (mean ± S.E., $n = 4$) (24).

cDNA. As shown in Fig. 1, *A* and *B* (*right panels*), cultivation at 26 °C for 24 h resulted in production of voltage-dependent macroscopic K^+ currents in both CHO and tsA 201 cells transfected with *eag* cDNA. Similar to Eag K^+ currents recorded from *Xenopus* oocytes, the whole-cell K^+ currents seen after growth at 26 °C were activated around −40 mV and exhibited open state inactivation at depolarized voltages. In addition, activation kinetics of the K^+ currents were slowed by either increasing the concentration of extracellular Mg^{2+} or applying a hyperpolarizing prepulse potential (29), both of which are characteristic features of Eag channels (28, 30).

To assess the effect of cultivation temperature on current expression of Eag channels, we measured whole-cell K^+ currents in *eag*-transfected CHO cells after cultivating at various temperatures for 24 h. As quantified by current density (pA/pF) at a depolarizing potential of +40 mV, macroscopic K^+ currents began to be restored by lowering cultivation temperature to 30 °C, whereas the largest augmentation of current level was observed at 26 °C (Fig. 1*C*). At 26 °C, restoration of macroscopic K^+ currents required cultivation of transfected cells for a minimum of 3 h, and the level of Eag K^+ currents was substantially increased by longer cultivation at the lower temperature (Fig. 1*C*). Consistent with these results, recording at room temperature for an extended period did not restore currents from cells cultivated at 37 °C, nor did acute up-shift of temperature to 37 °C during recordings affect the rate of rundown or abolish K^+ currents in cells grown at 26 °C (Fig. 1*D*). Together, these data suggest that temperature-dependent expression of Eag currents is not a direct effect of recording temperature on channel activation.

Surface Expression of Eag Channels Is Not Affected by Cultivation Temperatures—One explanation for the restoration of macroscopic K^+ currents by lower temperature could involve temperature sensitivity of the cell surface expression of the channel. To test this, we assessed the effect of culture temperature on plasma membrane targeting of Eag proteins using surface biotinylation with avidin pulldown to selectively harvest Eag proteins that were on the plasma membrane. Similar to previous reports, the anti-Eag antibody identifies two bands from both avidin pulldown and total cell lysates (Fig. 2*A*), corresponding to the full-length channel and an 80-kDa protein (Eag80), which was produced from a cryptic in-frame splicing event and occurs with transfections of the full-length *eag* cDNA (21). Surface expression of Eag channels was not

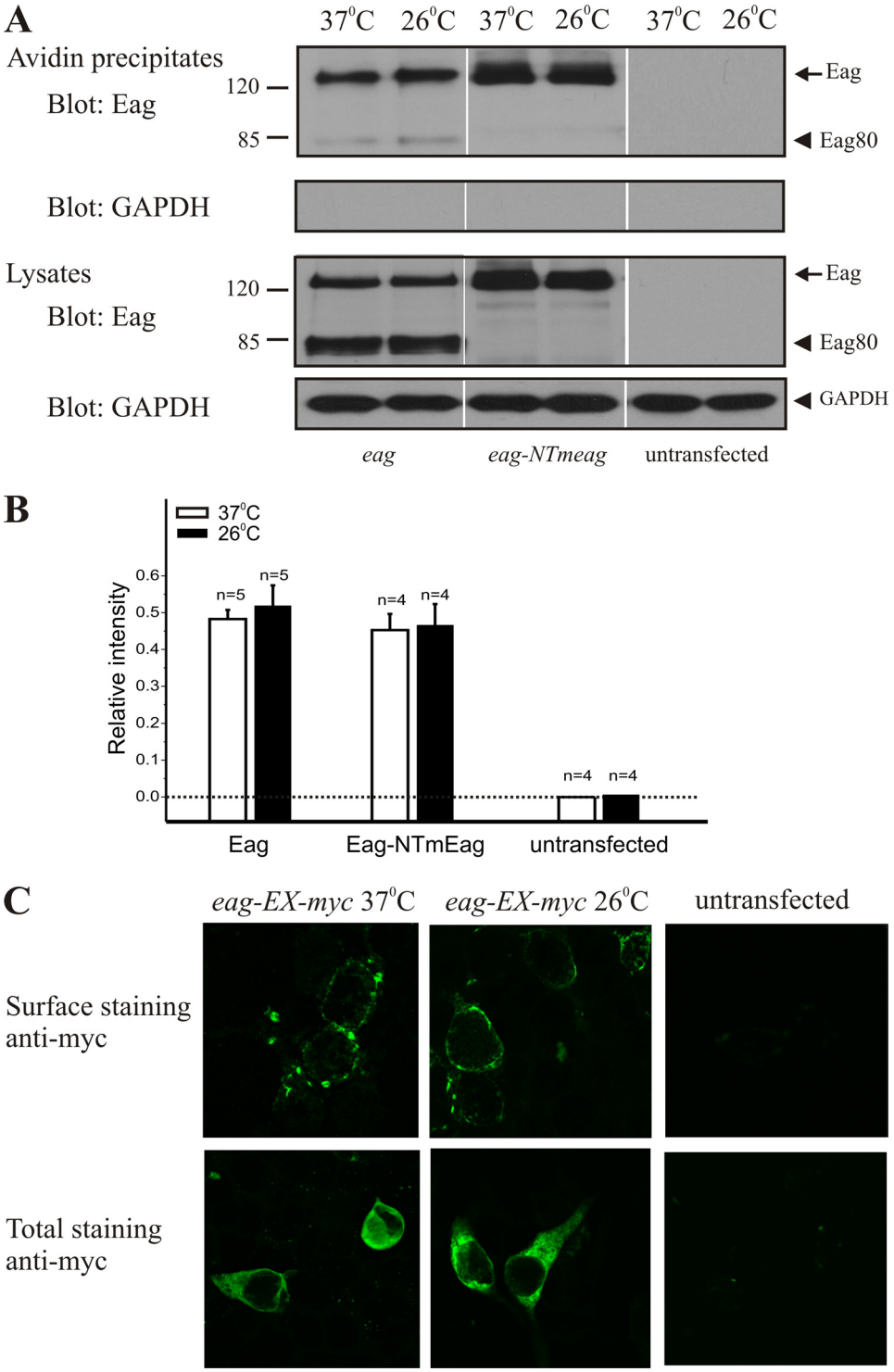

FIGURE 2. **Cultivation temperature does not affect cell surface targeting of Eag channels.** *A,* cell surface proteins were biotinylated using a membrane-impermeable reagent and isolated with streptavidin beads. Channel immunoreactivity in the streptavidin precipitates (*1st panel*) and in the lysates (*3rd panel*) was detected with an anti-Eag antibody that recognizes the EagCT. The biotinylation reagent did not label an intracellular protein, GAPDH (*2nd* and *4th panels*), confirming its specificity for cell surface proteins. *B,* temperature does not affect the proportion of Eag or Eag-NTmEag trafficked to the plasma membrane. Both Eag and Eag-NTmEag are targeted to the plasma membrane in similar proportion to cells cultivated at 37 °C (*white bars*) and 26 °C (*black bars*). Data are expressed as the ratio of arbitrary densitometry units from streptavidin precipitates and cell lysates as determined by densitometric analyses of immunoblots. *C,* confocal images of tsA 201 cells that were either untransfected or transfected with *eag*-EX-myc cDNA. Anti-Myc antibodies were used to label surface (*top panels*) and total Eag protein (*bottom panels*). Representative images from one of six independent experiments are shown.

affected by cultivation temperature, as the ratio of biotinylated Eag proteins to those in total lysates was not significantly different between cells cultivated at 26 and 37 °C (Fig. 2*B*). As a control, we also examined surface targeting of a chimeric Eag-NTmEag channel whose current expression was independent of cultivation temperature (see Fig. 5). For both Eag

and Eag-NTmEag, the full-length proteins are identically sized tight bands at 26 and 37 °C (Fig. 2*A*), suggesting that there was no temperature-dependent shift in the molecular weight of channel proteins in these cells that could reflect differential glycosylation or other maturation processes.

We next directly visualized the surface expression of Eag proteins using immunofluorescence. In these experiments, surface-targeted Eag channels were probed with an anti-Myc antibody that recognized a Myc epitope inserted on the extracellular side of the Eag channel and visualized with FITC-conjugated secondary antibody by confocal microscopy. In Fig. 2*C* (*top panels*), it can be seen that Eag channels were localized to the plasma membrane in transfected cells cultured at both 37 and 26 °C. When the cell membranes were permeabilized with nonionic detergent, we did not observe any significant difference in the cytoplasmic distribution of total Eag proteins between cells cultivated at 26 and 37 °C (Fig. 2*C*, *bottom panels*). Together, these data demonstrate that the temperature-dependent expression of K^+ channel currents cannot be attributed to a deficit in trafficking or surface targeting of Eag channels.

Voltage-dependent Gating Charge Movement of Eag K^+ Channels Is Not Affected by Cultivation Temperatures—Voltage-dependent opening of ion channels is a process that entails coordinated conformational changes of both the voltage sensor and the activation gate (4). To identify the defective step(s) that might have caused the failure to conduct K^+ ions when the Eag channel is assembled and targeted at 37 °C, we assessed the integrity of its voltage sensor by measuring voltage-dependent gating charge movements. To record Eag gating currents, we used intracellular and extracellular NMG^+ solutions to substitute for K^+ and Na^+ ions and applied a P/−4 voltage protocol to subtract capacitive and leak currents. As shown in Fig. 3*A*, on- and off-gating currents were elicited by depolarizing voltages in some *eag*-transfected CHO cells cultivated at either 26 or 37 °C. These were genuine gating currents of Eag channels, because they were not present in any untransfected or vector-transfected CHO cells (Fig. 3*B*) (31) and were similar in voltage dependence and kinetics to that of the Eag on- and off-gating currents previously recorded in oocytes (30, 32). However, unlike Shaker channels that exhibited ample gating currents in a majority of transfected cells, Eag gating currents had smaller amplitudes, and well resolved on- and off-gating currents were only detected above noise in a fraction of *eag*-transfected cells (Fig. 3*B*). Importantly, the percentage of cells that exhibited measurable gating currents was not different in transfected cells cultivated at the two temperatures (Fig. 3*B*), and a comparison of the charge-voltage relationship (Q-V) also revealed little difference between Eag gating currents recorded from cells cultivated at 26 and 37 °C (Fig. 3*C*).

We also recorded Eag gating currents using intracellular and extracellular solutions containing a K^+ channel blocker, TEA. In *eag*-transfected cells, this recording condition yielded sizeable on-gating but very small off-gating currents, which is consistent with the short pulse duration and the presence of TEA in these experiments (23, 30). Different from on-gating currents of Shaker K^+ channels, Eag on-gating currents were activated at higher depolarizing voltages and had a slower rising phase (Fig. 3*D*). The kinetics and voltage dependence of the on-gating currents were not significantly different for *eag*-transfected cells cultivated at 26 and 37 °C, confirming that

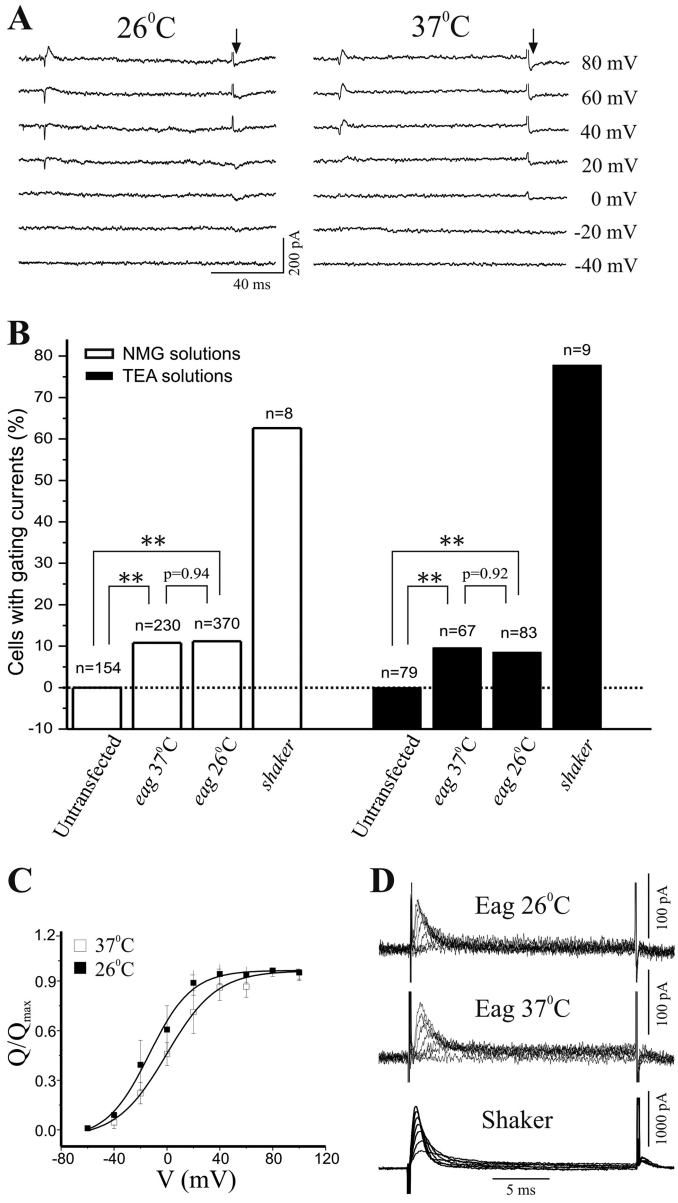

FIGURE 3. **Cultivation temperature does not affect gating currents of Eag channels.** *A,* representative gating current traces evoked by depolarizing voltages recorded in *N*-methyl-D-glucamine solutions from *eag*-transfected CHO cells cultivated at 26 °C (*left*) or 37 °C (*right*). The *arrows* indicate the region for obtaining off-gating charge movement (Q). *B,* summary of percentage of *eag*- or *shaker*-transfected CHO cells that exhibited measurable gating currents. No gating currents were detected from any untransfected CHO cell. There were statistically significant differences between untransfected and *eag*-transfected cells cultivated at either 26 or 37 °C (**, $p < 0.01$, logistic regression), although the probability of gating current occurrence was not different between cells grown at 26 or 37 °C (*p* values shown in *B*). *C,* normalized Q-V curve determined from *eag*-transfected cells cultivated at 26 or 37 °C. *Solid lines* represent fits of Boltzmann function. Fitted values of $V_{1/2}$ were -13.4 ± 7.2 mV, $n = 10$, in cells cultivated at 26 °C and -0.2 ± 6.9 mV, $n = 11$, in cells at 37 °C. $p > 0.05$ for the comparison of $V_{1/2}$ values between the two groups using one-way ANOVA. *D,* representative on-gating current traces recorded in TEA solutions from *eag*-transfected CHO-K1 cells cultivated at 26 °C (*top*) or 37 °C (*middle*). On-gating currents from *shaker*-transfected cells (*bottom*) were used for comparison.

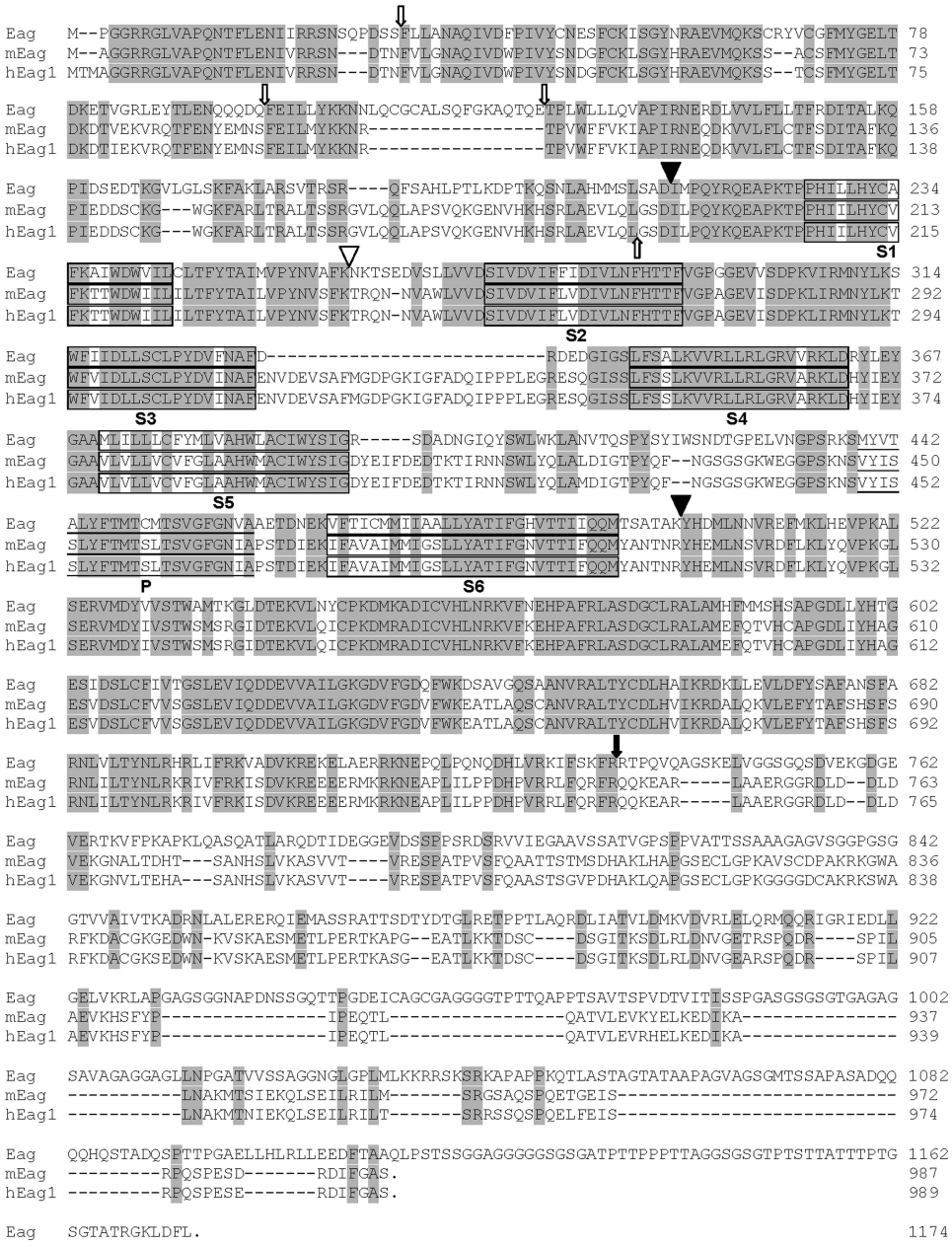

FIGURE 4. **Comparison of amino acid sequences of Eag, mEag, and hEag1.** Identical residues in the three channel proteins are shown in *shaded boxes* and predicted membrane-spanning regions are *outlined*. *Filled triangles* denote the positions of chimeric channel constructions and full C-terminal deletions. The sites of distal C-terminal truncation and internal Myc tag insertion are indicated with a *filled arrow* and *open triangle*, respectively. N-terminal truncations are indicated with *up* or *down open arrows* for mouse and fly channels, respectively.

cultivation temperatures did not affect voltage-dependent gating charge movements of the Eag channel.

Intracellular Terminal Regions Play a Significant Role in Structure and Function of Eag K^+ Channels—The Eag protein shares substantial homology with its mammalian counterparts (Fig. 4), but functional expression of other Eag homologues is not dependent on cultivation temperatures (14). To determine the potential role of various regions of the Eag channel in mediating temperature-dependent expression of functional K^+ channels, we employed a chimeric channel strategy. We first generated three chimeric channels (Eag-S1-S6mEag, Eag-CTmEag, and Eag-NTmEag) in which either the transmembrane (S1–S6), C-, or N-terminal domain of the Eag channel was replaced with the corresponding region of its mouse homologue, mEag (Fig. 4). *meag*-transfected cells have robust K^+ currents regardless of culture temperature (Fig. 5*A*). When either its NT or CT was replaced with mEag sequences, the temperature dependence of Eag current was alleviated. Robust K^+ currents were elicited from transfected cells at both temperatures (Fig. 5, *B* and *C*), although the current density was higher in cells maintained at 26 °C than that at 37 °C (Fig. 5*E*). In addition, the chimeric channels exhibited changes in their biophysical properties. The Eag-NTmEag channel had slower activation kinetics than wild-type Eag (supplemental Fig. S1*A*), whereas the Eag-CTmEag channel had an enhanced voltage sensitivity (Fig. 5*F*) and considerably

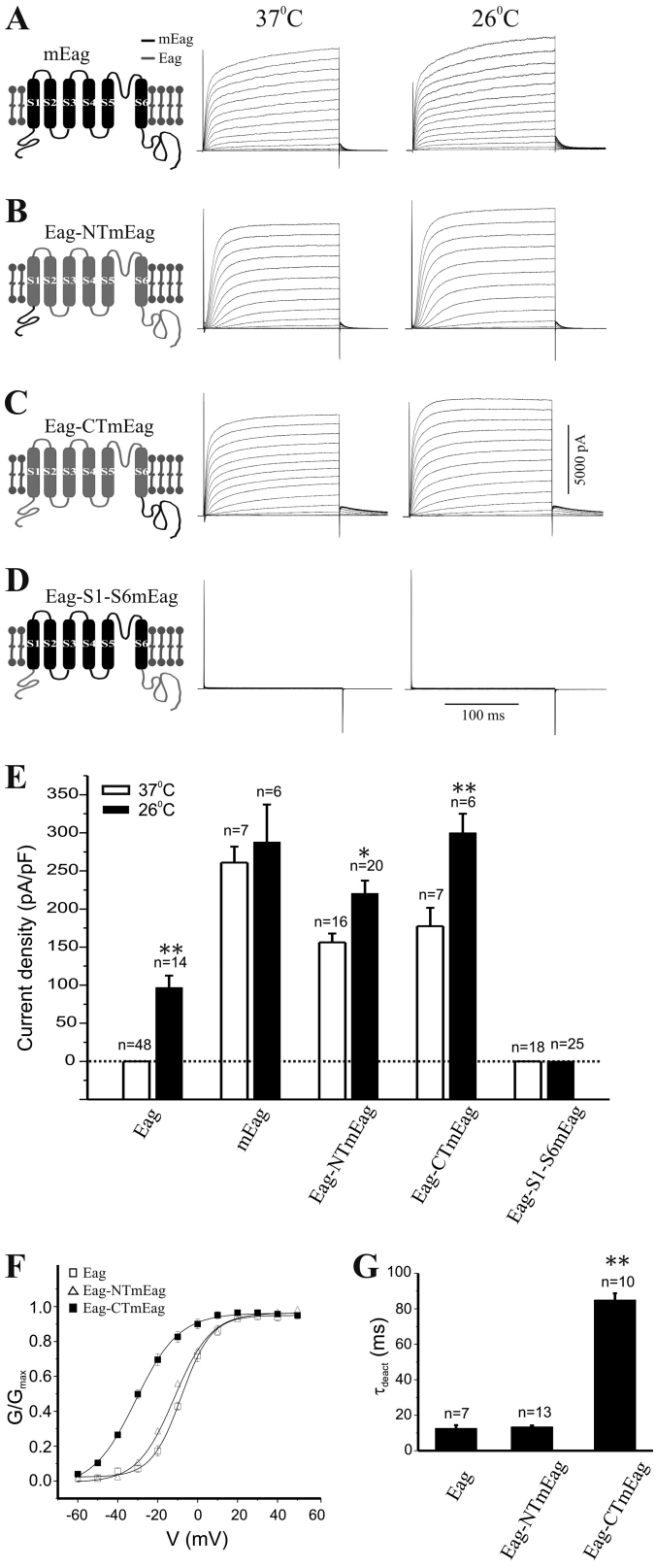

FIGURE 5. **Temperature-independent expression of chimeric Eag-mEag channels.** Schematics of chimeric channels are shown on the *left*. mEag is indicated in *black*, Eag in *gray*. Macroscopic K^+ currents were measured in cells cultivated at either 37 °C (*left*) or 26 °C (*right*) after transfection with cDNA for mEag (*A*) or the chimeric channels Eag-NTmEag (*B*), Eag-CTmEag (*C*) and Eag-S1-S6mEag (*D*). *E,* quantification of current density (mean ± S.E.) at +40 mV from CHO cells transfected with wild-type or various chimeric channels cultivated at either 37 or 26 °C (*, $p < 0.05$; **, $p < 0.01$, one-way ANOVA). *Dotted line* indicates current density of zero. Chimeric channels showed alterations in biophysical properties. *F,* plot of normalized conductance (G/G_{max}) as a function of voltage (*V*) determined from CHO cells cultivated at 26 °C that expressed Eag (*open square*), Eag-NTmEag (*open triangle*), or Eag-CTmEag (*filled square*) channels. The *G-V* curve of Eag-CTmEag channels has a significant left shift, indicating an increase in voltage sensitivity. *G,* comparison of the deactivation kinetics of Eag and the two chimeric channels, measured as the deactivation time constant (τ_{deact}) (mean ± S.E.). Unlike Eag-NTmEag, the Eag-CTmEag channel deactivates significantly slower than Eag (**, $p < 0.01$, one-way ANOVA).

slower deactivation kinetics than Eag and Eag-NTmEag channels (Fig. 5*G*).

One possible interpretation of the finding that replacement of either the NT or CT of Eag with mEag was sufficient to restore currents at 37 °C is that Eag channel assembly at high temperature disrupts some interaction between these two domains that blocks their ability to participate in allowing opening of the channel following movement of the voltage sensor. Substitution of the mEag NT or CT allows a functional interaction between terminal domains and rescues activation. To further probe the role of the interaction of the transmembrane domain with the intracellular domains in activation, we generated a chimeric channel that contained both the EagNT and CT attached to the mEag transmembrane domains. Although it was expressed at the cell surface (supplemental Fig. S2), the Eag-S1-S6mEag channel failed to produce any significant K^+ currents when it was transfected into mammalian cells cultivated at either 26 or 37 °C (Fig. 5, *D* and *E*). Hence, although this experiment confirmed the importance of intracellular domains for function, the failure of EagNT and CT domains to support activation of the mEag channel suggested that there were significant differences in how the TM regions interacted with their cognate intracellular domains.

Comparison of the fly and mouse Eag channels sequences reveals that only the proximal regions of their CT domains (amino acid residues 496–734 of Eag and 504–743 of mEag) show good conservation (Fig. 4). To test the differential roles of the distal and proximal CT domains, we generated Eag and mEag channels, which have a truncation of the distal CT sequence where Eag and mEag are least homologous (Fig. 4). Notably, none of the channels (mouse, fly, and chimera) that lack the distal CT domain produced current at 37 °C, and all had greatly reduced current amplitudes at 26 °C (Fig. 6; note difference in the *y* axis scale between Figs. 6*G* and 5*E*). This indicates a general role for the distal CT in modulation of current amplitude.

The distal CT also appeared to have additional functionality. When transfected into mammalian cells, the EagΔ735–1174 channel was not much different from the full-length wild-type channel in its temperature-dependent conduction of K^+ ions (Fig. 6*A*). In contrast, this C-terminal deletion converted the nonconducting chimeric channels that had the mEag transmembrane domains into an Eag-like K^+ channel. Eag-S1-S6mEagΔ735–1174 channels produced macroscopic K^+ currents but only when the transfected cells were cultivated at lower temperatures (Fig. 6*B*), implying that the distal CT was responsible for the inability of the Eag-TMmEag channel (Fig. 5*D*) to conduct K^+.

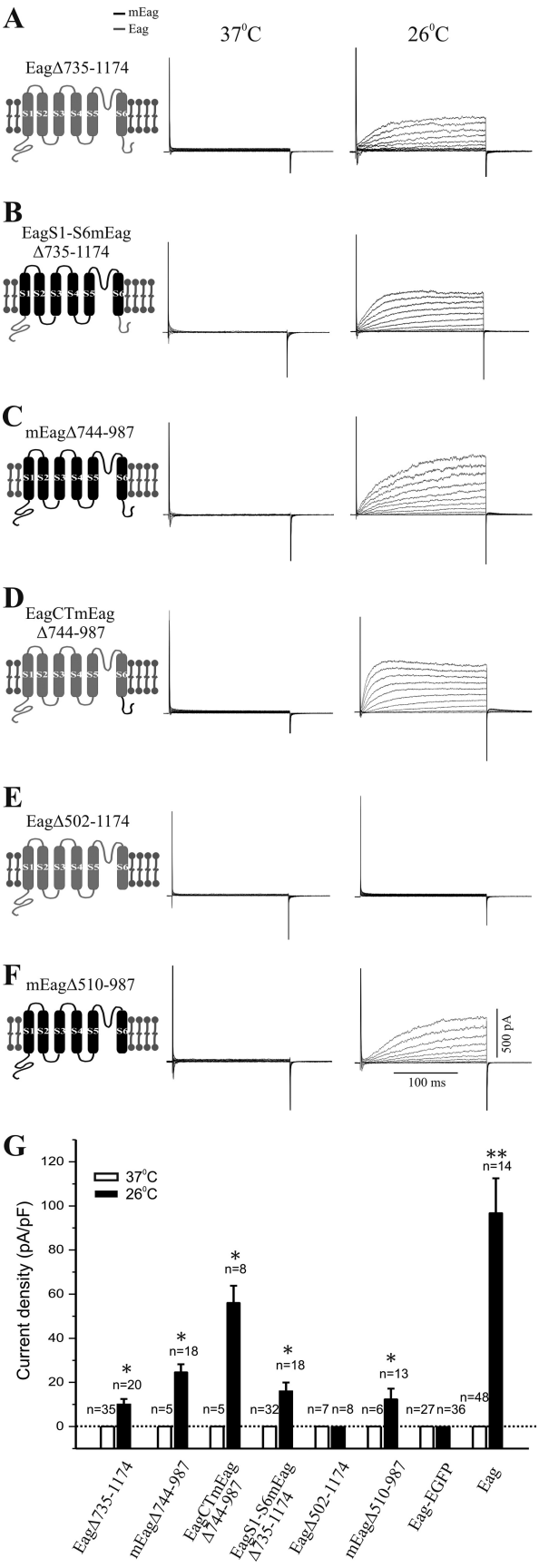

FIGURE 6. **Importance of CT domain in the functional expression of Eag channels.** Schematics of mutant channels are shown on the *left*. mEag is indicated in *black* and Eag in *gray*. Macroscopic K^+ currents were recorded from cells grown at 37 °C (*left*) or 26 °C (*right*) after transfection with cDNA encoding Eag Δ735–1174, the Eag protein with a deletion of its distal CT domain (amino acids 735–1174) (*A*), Eag-S1-S6mEag Δ735–1174, the mEag transmembrane domain attached to Eag intracellular domains with a deletion of the distal CT domain (amino acids 735–1174) (*B*), mEag Δ744–987, the mEag protein with a deletion of its distal CT domain (amino acids 744–987) (*C*), Eag-CTmEag Δ744–987, the mEag CT domain attached to EagNT and transmembrane domains with a deletion of the distal CT domain (amino acids 744–987) (*D*), Eag Δ502–1174, the Eag protein with a deletion of its entire CT domain (amino acids 502–1174) (*E*), and mEag Δ510–987, the mEag protein with a deletion of its entire CT domain (amino acids 510–987) (*F*). *G*, quantification of current density (mean ± S.E.) at +40 mV from CHO cells transfected with various CT-truncated or EGFP-tagged channels cultivated at either 37 or 26 °C (*, $p < 0.01$, one-way ANOVA). Data of wild-type Eag channels were included for comparison. *Dotted line* indicates current density of zero. Note that no current was expressed when Eag protein was fused with a C-terminal EGFP-tag.

Interestingly, after a deletion of the equivalent distal C-terminal region, the two temperature-independent channels, mEag and Eag-CTmEag, became temperature-sensitive, as both mEagΔ744–987 and Eag-CTmEagΔ744–987 only generated K^+ currents when cultivated at lower temperatures (Fig. 6, *C* and *D*), suggesting another role for the distal CT in stabilization of the NT/proximal CT interaction. Removal of the entire CT domain (Eag Δ502–1174) rendered the fly Eag channel nonconductive at either temperature (Fig. 6*E*). In contrast, the mutant mEag channel devoid of the C-terminal tail (mEagΔ510–987) was capable of producing a low level of macroscopic K^+ currents at 26 °C (Fig. 6*F*). The proximal CT domain appears to be absolutely required in the fly but not in the mouse for ion conductance. In addition, these CT-truncated mutant channels had slower activation kinetics when compared with the respective full-length channels (supplemental Fig. S1*B*), indicating an involvement of CT domains in channel biophysical property.

We also examined the role of the NT domain in current expression by constructing mutant Eag and mEag channels, which have truncations of their N-terminal regions. Previously, it had been reported that, when expressed in *Xenopus* oocytes, NT-truncated rat Eag and hERG channels produce functional K^+ currents with altered activation or inactivation properties (33), which can be restored by co-expression of a recombinant N-terminal domain (34, 35). When transfected into CHO cells cultivated at 37 °C, the NT-truncated mutant mEag channel (mEagΔ2–188) yielded very small currents; only 6 in 14 transfected cells exhibited detectable macroscopic currents with an average current density of 5.77 pA/pF (Fig. 7*B*). Current levels in cells transfected with mEagΔ2–188 were significantly enhanced by cultivating cells at lower temperature; the average current density increased to 35.01 pA/pF in cells cultivated at 26 °C.

We next tested the effect of a recombinant mEag NT domain on the NT-truncated mEag channel. As shown in Fig. 7*D*, co-expression of mEagΔ2–188 and mEagNT1–190 in cells cultivated at 26 °C led to generation of robust K^+ currents, which were similar to wild-type mEag in both current density and deactivation kinetics. Intriguingly, the enhancement of current expression by mEag NT domain was not observed in cells cultivated at 37 °C (Fig. 7*D*, *left trace*).

The NT domain of Eag is largely homologous with that of mEag (Fig. 4). In this study, we generated three mutant Eag

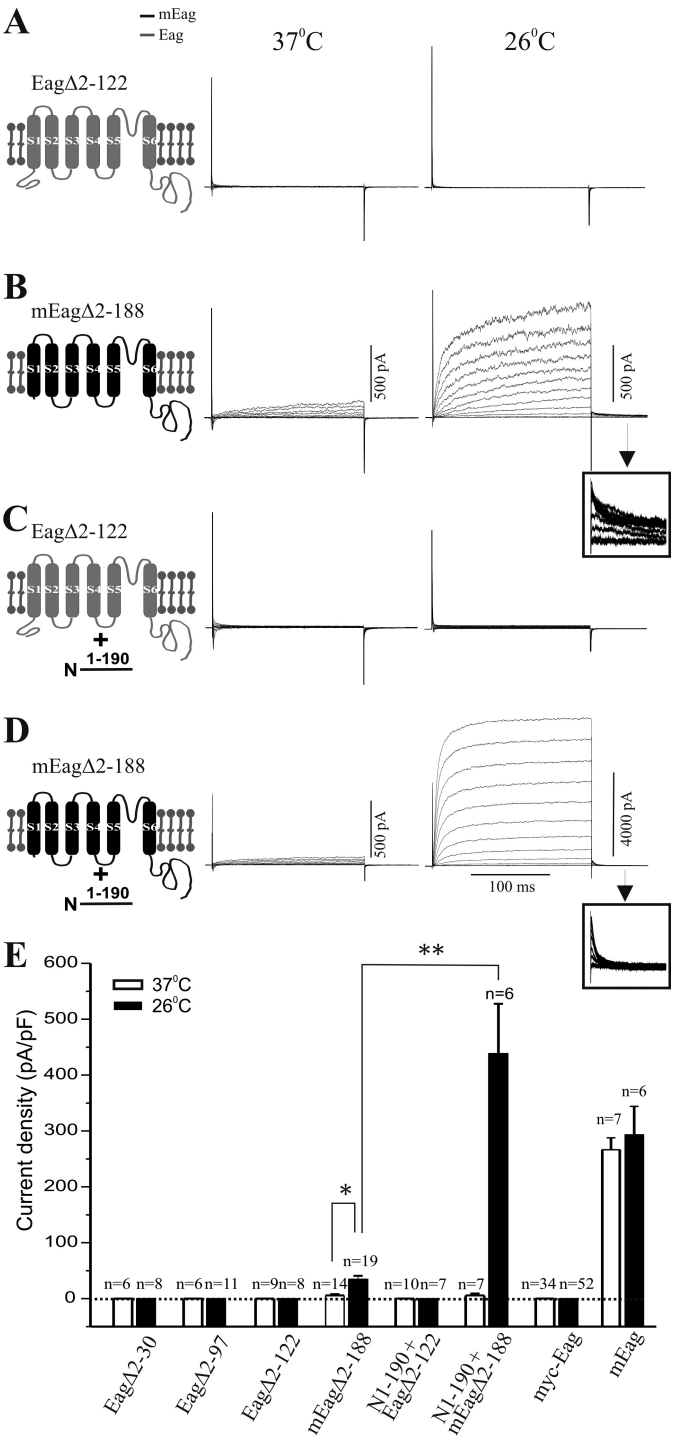

FIGURE 7. **Importance of NT domain in the functional expression of Eag channels.** Schematics of mutant channels are shown on the *left*. mEag is indicated in *black* and Eag in *gray*. Macroscopic K^+ currents were recorded from cells grown at 37 °C (*left*) or 26 °C (*right*) after transfection with cDNA encoding Eag Δ2–122, the Eag protein with a deletion of its distal NT domain (aa 2–122) (*A*), mEag Δ2–188, the mEag protein with a deletion of its entire NT domain (amino acids 2–188) (*B*), and Eag Δ2–122 plus mEagNT1–190-HA, the mEag NT domain fused with an HA tag (*C*), and mEag Δ2–188 plus mEagNT(1–190)-HA (*D*). *Insets* in *B* and *D* are expanded tail currents showing their different deactivation kinetics. *E*, quantification of current density (mean ± S.E.) at +40 mV from CHO cells transfected with various NT truncated or N-terminal Myc-tagged channels cultivated at either 37 or 26 °C (*, $p < 0.05$; **, $p < 0.01$, one-way ANOVA). Data of wild-type mEag channels were included for comparison. *Dotted line* indicates current density of zero. Note that no current was expressed when Eag protein was fused with six N-terminal Myc tags.

channels that are truncated at amino acids 30, 97, and 122 of its NT domain. Using biochemical approaches, we verified that these mutant channel proteins were expressed and targeted to the cell surface (supplemental Fig. S2). However, they failed to produce any K^+ currents in transfected CHO cells (Fig. 7*A*) nor did co-expression of the recombinant mEag NT domain restore current expression at different cultivation temperatures (Fig. 7*C*). Thus, integrity of the EagNT domain appears to be critical for its functional expression.

To obtain additional evidence in support of the role of the EagNT and CT domain interaction in channel activation processes, we examined the effect of N- or C-terminal tagging on Eag channel conductivity. Addition of such protein tags can disrupt native interactions in proteins (36, 37). As shown in Figs. 6*G* and 7*E*, no voltage-activated K^+ current was recorded in cells that were transfected with either a tandem of six N-terminal Myc (myc-Eag) or a C-terminal EGFP (Eag-EGFP)-tagged channel. The failure of conduction was not caused by a deficit in surface expression (supplemental Fig. S2) and could not be rescued by lowering the cultivation temperature to 26 °C. This is consistent with a previous report showing that a similar Myc-tagged Eag channel construct produces detectable gating currents but not outward K^+ currents when expressed in *Xenopus* oocytes (38). These results indicate that addition of amino acids to either the NT or CT of the *Drosophila* Eag channel is sufficient to disrupt their functional interaction.

DISCUSSION

The *Drosophila* Eag channel was originally identified based on the phenotype of a mutant with ether-induced leg-shaking (39). This led to the discovery of a family of related K^+ channels with a variety of biological functions (13). However, unlike most other families of K^+ channels cloned from *Drosophila,* Eag channels fail to produce voltage-dependent K^+ currents in cultured mammalian cells, a widely used heterologous expression system that is advantageous for both biochemical and electrophysiological studies of ion channels. In this study, we demonstrate that the Eag channel can be functionally expressed in mammalian cell lines at lower cultivation temperatures. We show that voltage-dependent gating charge movements are preserved for Eag channels assembled and targeted at 37 °C. Therefore, absence of K^+ currents in these channels has to be caused by a defect in one of the subsequent processes, such as coupling between voltage sensor and activation gate and opening of the ion conduction pore (4, 8).

The mechanism by which lower cultivation temperature restores Eag channel functions appears to be a novel one. It is known that reducing culture temperature can facilitate surface expression of trafficking-defective membrane proteins, including mutant cystic fibrosis transmembrane regulator and hERG channels (26, 40). Using both biochemical and immunocytochemical approaches, we have determined that surface expression of Eag proteins is not significantly affected by cultivation temperatures. Temperature may affect many other steps of channel protein biogenesis, including hydrophobic interactions in protein folding (16, 41, 42). Once Eag channels are inserted into the plasma membrane, however, their con-

formations are minimally affected by temperature, because Eag K^+ currents persist when recorded at 37 °C, and restoring K^+ currents requires cultivation of transfected cells at a lower temperature for several hours, which presumably reflects time required for new channel biogenesis and assembly. The fact that gating charge movements of Eag channels were independent of cultivation temperature suggests that the positioning of the TM domains that include the voltage sensor is intact. This raises the possibility that the temperature dependence of Eag channel properties is reporting a difference in the conformation of Eag intracellular domains or their interface with the TM domains. Hence, our results provide an apparent example of subtle temperature-dependent effects on potassium channel biosynthesis and assembly, in contrast to the more usual catastrophic effects of misfolding, which result in complete retention of nascent channel proteins in the endoplasmic reticulum or Golgi.

The ability of the structure of the NT and CT domains to confer both temperature sensitivity and to activate ion conductance indicates that these domains have a critical role in regulation of Eag activity. Our results suggest a model in which the N and proximal C termini of Eag interact with each other to regulate channel activation. This regulatory function is disrupted by folding at 37 °C, a temperature not normally experienced by this protein because *Drosophila melanogaster* is not viable for long in this temperature range. Interestingly, removal of particular domains of mEag can also generate a temperature-sensitive channel, suggesting that these NT/CT interactions are a conserved feature of this family. Our assessment of multiple deletion and chimeric channels indicates that the temperature sensitivity of Eag does not map to a specific residue or domain, but rather it appears to be due to a failure at the level of domain interaction. These analyses also point to specific functions for the NT, proximal CT, and distal CT domains in this collaboration.

Sequences in the unconserved distal CT functionally distinguish between fly and mouse TM domains, perhaps implying that residues within the TM domains or in the short intracellular loops are critical for brokering the effects of the intracellular domains on activation. The distal CT is also clearly involved in modulation of current amplitude, because all channels that lack this subdomain have substantially reduced amplitudes. The ability of deletion of the distal CT to make mEag temperature-sensitive might suggest a third role as a stabilizer for NT/proximal CT/channel interactions at higher temperatures. The proximal CT, on the other hand, appears to have disparate roles in the mouse and the fly. In the fly channel it is absolutely required, whereas mEag channels that lack all CT sequences can still pass small currents. This perhaps is consistent with a role for this subdomain to help position the NT domain for channel activation.

The role of the NT domain also differs between Eag and mEag. It is absolutely required in the fly channel, because even small deletions abolish currents. mEag channels lacking this domain are still able to pass current but do so with greatly decreased amplitudes, especially at 37 °C. Providing the mEag NT in *trans* fully rescues NT-less mEag at 26 °C but not at 37 °C. Co-expression of mEag NT does not reinstate the ability of NT-less Eag to conduct ions. This differential rescue supports a model that full coupling of gating to activation requires a multidomain complex of the NT and CT and would be consistent with the idea that the intrinsic binding of these domains in Eag is weaker than in mEag. When the NT is attached to the Eag or mEag channel domain, it is in a very high local concentration, and this drives binding between NT and CT. When the NT is provided as a separate protein, its interaction with the CT is now diffusion-limited. In the case of the mouse channel at low temperatures, the complex is stable and you see current at 26 °C. Higher temperatures destabilize the complex. In the case of the fly channel, the NT/CT binding is very weak and unstable in the diffusion-limited case even at 26 °C. This would make the prediction that driving binding by providing very high levels of mEag NT in *trans* might rescue the NT-less Eag. The hypothesized differential temperature sensitivities of the fly and mouse NT/CT interactions could be a reflection of the different temperatures normally experienced by temperate-living poikilotherms and warm-blood homeotherms.

The coupling of gating to activation is not the only role for these intracellular domains. Our studies using chimeric Eag-mEag channels also revealed significant contributions of the NT and CT regions to determine both the voltage dependence of activation and activation and deactivation kinetics, confirming that these intracellular regions are integral to multiple aspects of Eag channel function (43).

Intrigued by the temperature-dependent functional expression of Eag channels, we have identified an important role of the intracellular domains in Eag channel structure and function. Future studies using more sophisticated methodologies should be able to pin down the temperature-sensitive interactions, and thus gain insight into the molecular details of Eag channel activation. As the NT and CT regions are sites of interactions for several regulatory proteins, our findings may shed some light on the functional significance of these modulatory protein complexes. In particular, they may bear some relevance to the signaling roles of Eag family channels that are suggested to correlate with channel conformation and the state of activation (38, 44, 45). On the other hand, our data may help to elucidate certain types of channelopathies resulting from production of nonconducting channels that are trafficked to the plasma membrane. This is particularly applicable to human long QT syndrome, which can be caused by defective activation of hERG channels because of mutations in the intracellular domains of the channel protein. Moreover, our findings may provide a potential model for nonconducting Eag-like channels induced by environmental stress, such as higher temperatures experience by patients at pathological conditions.

Acknowledgments—We thank Dr. Zheng Wang for helpful suggestions, Dr. Gisela Wilson for providing eag cDNA plasmids, Ruth Didier of the Florida State University Confocal Facility for help with imaging, and Rani Dhanarajan and Cheryl Pye of the Molecular Core Facility at Florida State University for generating some of the mutant cDNA constructs.

REFERENCES

1. Jan, L. Y., and Jan, Y. N. (1997) *Annu. Rev. Neurosci.* **20,** 91–123
2. Jiang, Y., Lee, A., Chen, J., Cadene, M., Chait, B. T., and MacKinnon, R. (2002) *Nature* **417,** 523–526
3. Wray, D. (2009) *Eur. Biophys. J.* **38,** 271–272
4. Tombola, F., Pathak, M. M., and Isacoff, E. Y. (2006) *Annu. Rev. Cell Dev. Biol.* **22,** 23–52
5. Levitan, I. B. (2006) *Nat. Neurosci.* **9,** 305–310
6. Jiang, Y., Lee, A., Chen, J., Cadene, M., Chait, B. T., and MacKinnon, R. (2002) *Nature* **417,** 515–522
7. Wray, D. (2004) *Eur. Biophys. J.* **33,** 194–200
8. Lu, Z., Klem, A. M., and Ramu, Y. (2002) *J. Gen. Physiol.* **120,** 663–676
9. Warmke, J. W., and Ganetzky, B. (1994) *Proc. Natl. Acad. Sci. U.S.A.* **91,** 3438–3442
10. Perrin, M. J., Subbiah, R. N., Vandenberg, J. I., and Hill, A. P. (2008) *Prog. Biophys. Mol. Biol.* **98,** 137–148
11. Ganetzky, B., and Wu, C. F. (1983) *J. Neurogenet.* **1,** 17–28
12. Griffith, L. C., Wang, J., Zhong, Y., Wu, C. F., and Greenspan, R. J. (1994) *Proc. Natl. Acad. Sci. U.S.A.* **91,** 10044–10048
13. Ganetzky, B., Robertson, G. A., Wilson, G. F., Trudeau, M. C., and Titus, S. A. (1999) *Ann. N.Y. Acad. Sci.* **868,** 356–369
14. Bauer, C. K., and Schwarz, J. R. (2001) *J. Membr. Biol.* **182,** 1–15
15. Jenke, M., Sánchez, A., Monje, F., Stühmer, W., Weseloh, R. M., and Pardo, L. A. (2003) *EMBO J.* **22,** 395–403
16. Brown, C. R., Hong-Brown, L. Q., and Welch, W. J. (1997) *J. Clin. Invest.* **99,** 1432–1444
17. Wilson, G. F., Wang, Z., Chouinard, S. W., Griffith, L. C., and Ganetzky, B. (1998) *J. Biol. Chem.* **273,** 6389–6394
18. Marble, D. D., Hegle, A. P., Snyder, E. D., 2nd, Dimitratos, S., Bryant, P. J., and Wilson, G. F. (2005) *J. Neurosci.* **25,** 4898–4907
19. Wang, Z., Wilson, G. F., and Griffith, L. C. (2002) *J. Biol. Chem.* **277,** 24022–24029
20. Sun, X. X., Hodge, J. J., Zhou, Y., Nguyen, M., and Griffith, L. C. (2004) *J. Biol. Chem.* **279,** 10206–10214
21. Sun, X. X., Bostrom, S. L., and Griffith, L. C. (2009) *Mol. Cell. Neurosci.* **40,** 338–343
22. Li, Y., Wu, Y., and Zhou, Y. (2006) *Neuron* **51,** 755–771
23. Perozo, E., MacKinnon, R., Bezanilla, F., and Stefani, E. (1993) *Neuron* **11,** 353–358
24. Robertson, G. A., Warmke, J. M., and Ganetzky, B. (1996) *Neuropharmacology* **35,** 841–850
25. Lansdell, S. J., Schmitt, B., Betz, H., Sattelle, D. B., and Millar, N. S. (1997) *J. Neurochem.* **68,** 1812–1819
26. Zhou, Z., Gong, Q., and January, C. T. (1999) *J. Biol. Chem.* **274,** 31123–31126
27. Szabò, I., Negro, A., Downey, P. M., Zoratti, M., Lo, Schiavo, F., and Giacometti, G. M. (2000) *Biochem. Biophys. Res. Commun.* **274,** 130–135
28. Yang, K., Fang, K., Fromondi, L., and Chan, K. W. (2005) *FEBS Lett.* **579,** 4113–4118
29. Liu, X., Wu, Y., and Zhou, Y. (2010) *Channels* **4,** 311–318
30. Tang, C. Y., Bezanilla, F., and Papazian, D. M. (2000) *J. Gen. Physiol.* **115,** 319–338
31. Suda, N., Franzius, D., Fleig, A., Nishimura, S., Bödding, M., Hoth, M., Takeshima, H., and Penner, R. (1997) *J. Gen. Physiol.* **109,** 619–631
32. Bannister, J. P., Chanda, B., Bezanilla, F., and Papazian, D. M. (2005) *Proc. Natl. Acad. Sci. U.S.A.* **102,** 18718–18723
33. Terlau, H., Heinemann, S. H., Stühmer, W., Pongs, O., and Ludwig, J. (1997) *J. Physiol.* **502,** 537–543
34. Morais Cabral, J. H., Lee, A., Cohen, S. L., Chait, B. T., Li, M., and Mackinnon, R. (1998) *Cell* **95,** 649–655
35. Gustina, A. S., and Trudeau, M. C. (2009) *Proc. Natl. Acad. Sci. U.S.A.* **106,** 13082–13087
36. Zhang, J., and Crandall, I. (2007) *Lipids Health Dis.* **6,** 24
37. Schmeisser, H., Kontsek, P., Esposito, D., Gillette, W., Schreiber, G., and Zoon, K. C. (2006) *J. Interferon Cytokine Res.* **26,** 866–876
38. Hegle, A. P., Marble, D. D., and Wilson, G. F. (2006) *Proc. Natl. Acad. Sci. U.S.A.* **103,** 2886–2891
39. Warmke, J., Drysdale, R., and Ganetzky, B. (1991) *Science* **252,** 1560–1562
40. Brown, C. R., Hong-Brown, L. Q., and Welch, W. J. (1997) *J. Bioenerg. Biomembr.* **29,** 491–502
41. Baldwin, R. L. (1986) *Proc. Natl. Acad. Sci. U.S.A.* **83,** 8069–8072
42. Dill, K. A., Ozkan, S. B., Shell, M. S., and Weikl, T. R. (2008) *Annu. Rev. Biophys.* **37,** 289–316
43. Ju, M., and Wray, D. (2006) *Biochem. Biophys. Res. Commun.* **342,** 1088–1097
44. Pardo, L. A., del Camino, D., Sánchez, A., Alves, F., Brüggemann, A., Beckh, S., and Stühmer, W. (1999) *EMBO J.* **18,** 5540–5547
45. Stühmer, W., Alves, F., Hartung, F., Zientkowska, M., and Pardo, L. A. (2006) *FEBS Lett.* **580,** 2850–2852
46. Yu, S. P., and Kerchner, G. A. (1998) *J. Neurosci. Res.* **52,** 612–617